INTL JOURNAL OF ELECTRONICS AND TELECOMMUNICATIONS, 2024, VOL. 70, NO. 3, PP. 563-568
Manuscript received June 17, 2024; revised July, 2024. doi: 10.24425/ijet.2024.149579

Experimental validation of asymmetric PZT optimal shape in the active vibration reduction of triangular plates

Romuald Kuras, and Sebastian Hajder

***Abstract*—In the active vibration reduction of two-dimensional structures, piezoelectric actuators of regular shapes, e.g. rectangular, circular, are commonly used. However, the shape of the transducers can be irregular, asymmetric (a-PZT), and its geometry can be an object for optimization. The paper presents an experimental validation of the application of optimal shaped a-PZT in the active reduction of triangular plate vibrations. Optimization was based on the criterion of the maximum bending moment. This means that the center of a-PZT is located at the point where the bending moment of the plate has reached its absolute maximum. The isosceles right triangular plate with simply supported edges was chosen as the research object. The research confirms the validity of the criterion used for optimization and may be an introduction to considering the use of optimal a-PZT in the active reduction of vibrations for more complex structures.**

***Keywords*—triangular plate, active vibration reduction, AVC, open-loop control**

I. Introduction

MECHANICAL vibrations of the structure may affect its damage or expose people to direct or indirect danger. To reduce unwanted vibrations, passive and active methods are used. In the group of active methods, a new branches can be specified according to the type of actuator used. One of the commonly used actuators in active vibration reduction is the piezoelectric actuator.

There are many research papers in which PZT has been used to reduce vibrations. The effectiveness of vibration reduction is influenced by many factors related to the actuator, e.g. the place of its gluing on the structure or the voltage supplying the transducer. The geometry of the PZT is also significant. In [1] Wang presented optimization procedure of electrode shape for piezoelectric composite transducers. This approach improves actuator performance. In this research, actuators with regular shapes were studied, while the shape of the electrode was irregular. Zhang et. al. [2] investigated topology optimization of the electrode coverage over PZT patches. As the objective function was taken the total energy consumption so the goal was to find the minimum amount of energy that would provide a given level of vibration reduction. Another trend in the use of PZT for active vibration reduction are MFC actuators. MFC actuators – just like common PZT transducers – can be manufactured in any shape. Hence, the shape optimization procedure for this type of actuators would also be reasonable. Leniowska and Mazan [3] used MFC star-shaped actuators to suppress vibrations of a circular plate. MFC actuators were also studied by Rzepecki et al. [4] in a semi-active system to reduce vibrations of a rectangular plate. Donoso and Sigmund [5] presented the optimization of the width and thickness of the actuator in the active reduction of beam vibrations. The work assumes that the PZT layer covers the entire beam, so the piezoelectric material is distributed along the length of the structure. The thickness of the PZT was considered in terms of the thickness of the actuator layers. Wiciak and Trojanowski [6],[7] numerically investigated piezoelectric sensor-actuator hybrid for different shapes of the actuator/sensor parts. The tested shapes were square- or disc-based with a hole cut out for the sensor.

The paper aims to experimentally investigate the influence of various shapes of piezoelectric actuators on the effectiveness of vibration reduction. For this purpose, the parameters of the open-loop frequency response function were used. It was indicated which shape of the PZT - from among the selected ones - is the most effective. Actuators with standard and commonly used shapes were selected for comparison: square (s-PZT) and circular (c-PZT). The third PZT compared was defined as the asymmetric actuator (a-PZT). The theoretical model of a-PZT was initially presented for the one-dimensional case (beam vibrations) in [8], and then extended to plate vibrations in [9]. The shape of a-PZT results from analytical and numerical calculations presented in [9].

II. Theory

The governing equation of transverse vibration of triangular plate is based on Kirchhoff's classical small deflection theory [10], [11],

$$D\nabla^4 w(x,y,t) + \varrho h \frac{\partial^2 w(x,y,t)}{\partial t^2} = f(x,y,t) \qquad (1)$$

In the steady state the equation takes the form [10],

$$D\nabla^4 w(x,y) - \frac{\varrho h \omega_f^2}{D} w(x,y) = f(x,y) \qquad (2)$$

where f – external forces, w – transverse displacement of the plate, ω_f – excited frequency, ϱ – density of the plate,

R. Kuras is with Faculty of Electrical and Computer Engineering, Rzeszow University of Technology, Rzeszow, Poland (e-mail: r.kuras@prz.edu.pl).

S. Hajder is with Faculty of Electrical and Computer Engineering, Rzeszow University of Technology, Rzeszow, Poland (e-mail: s.hajder@prz.edu.pl).

h– thickness, $D = \frac{Eh^3}{12(1-\nu^2)}$ – flexural rigidity, E – Young's modulus, ν – Poisson's ratio of the plate.

The subject of the research was simply supported right triangular plate, so the boundary conditions can be expressed as,

$$\begin{aligned} w(x,y) = M_x(x,y) = 0 \quad &\text{for} \quad x = 0 \\ w(x,y) = M_y(x,y) = 0 \quad &\text{for} \quad y = 0 \\ w(x,y) = M_h(x,y) = 0 \quad &\text{for} \quad y = 1 - x \end{aligned} \tag{3}$$

where $M_x = -D\left(\frac{\partial^2 w}{\partial x^2} + \nu\frac{\partial^2 w}{\partial y^2}\right)$, $M_y = -D\left(\frac{\partial^2 w}{\partial y^2} + \nu\frac{\partial^2 w}{\partial x^2}\right)$, and the expression for M_h is the bending moment along the hypotenuse, $M_h = -D\left(\frac{\partial^2 w}{\partial h^2} + \nu\frac{\partial^2 w}{\partial n^2}\right)$, h – axis along the hypotenuse, n – axis perpendicular to the hypotenuse.

An external excitation is in the following form

$$f(x,y) = f_0\delta(x - x_0, y - y_0) \tag{4}$$

where f_0 – amplitude of the exciting force, $\mathbf{x_0} = (x_0, y_0)$ – point of applying the exciting force.

The free vibration problem was solved by the superposition method presented in [12]–[15]. The simply supported right triangular plate case is the subject of [14] and the calculated eigenvalues are exactly the same as in the mentioned article.

III. Model of a-PZT

The PZT-plate interaction model for a rectangular and circular actuator is commonly known and presented, for example, in [16]–[19]. The theoretical model of the asymmetric actuator results from the assumption that the arms of the a-PZT (and thus also the arms of the pairs of forces) are not equal and the second assumption: both moments of the pairs of forces are equal [8], [20]. This makes an asymmetry in the structure of the a-PZT. An important conclusion of the aforementioned papers is also the indication of a new criterion in the problem of location the actuator on a vibrating structure. In the case of asymmetrical vibrations, it is justified to use the maximum bending moment criterion, i.e. the point connecting both actuator arms should be located at the point where the bending moment reaches its absolute extreme.

Optimization of the length of each arm for the one-dimensional case does not change the shape of the actuator, but only the location of its edges in relation to the point of the maximum bending moment. However, for the two-dimensional case, the optimization of each actuator cross-section (in other words: each PZT fiber) leads to an irregular, asymmetric shape of the a-PZT, which will most effectively reduce the vibrations of the structure. The process of a-PZT construction from PZT fibers is shown in Fig. 1.

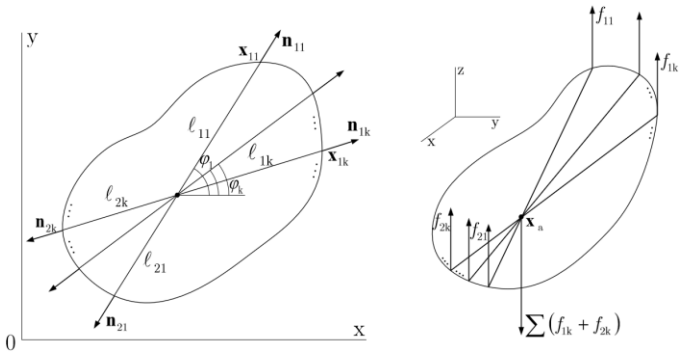

Fig. 1. The idea of constructing a-PZT

The model of the interaction of arbitrary a-PZT fiber on the plate can be described by,

$$2M_k = M_{1k} + M_{2k} = f_{1k}\ell_{1k} + f_{2k}\ell_{2k} \tag{5}$$

where ℓ_{1k}, ℓ_{2k} are the arm lengths of the asymmetric fibre.

The bending moments can be written as two pairs of forces,

$$\begin{aligned} M_{1k} + M_{2k} = f_{1k}\delta(x - x_{1k}, y - y_{1k}) + \\ -(f_{1k} + f_{2k})\delta(x - x_a, y - y_a) + \\ f_{2k}\delta(x - x_{2k}, y - y_{2k}) \end{aligned} \tag{6}$$

where k – number of PZT fibres in the a-PZT, f_{1k}, f_{2k} – forces due to a fibre, $(x_{1;k}, y_{1;k}), (x_a, y_a), (x_{2;k}, y_{2;k})$ – points of applying forces of a fibre.

The interaction of one a-PZT fiber on the plate is described by Eq. (6). To describe the interaction of the complete actuator on the plate, the actions from all fibers must be summed up. The theory of obtaining an asymmetric a-PZT shape for a two-dimensional structure is described in detail in [9].

Based on the pattern of the asymmetric actuator consisting of PZT fibers, three shapes of transducers were determined (see Fig. 2). The sum of the lengths of all fibers was constant for each case, the values of the bending moments were the same. The asymmetry of the arm length of each fiber was optimized. The place of gluing the actuator on the surface of the plate is shown in the Fig. 3.

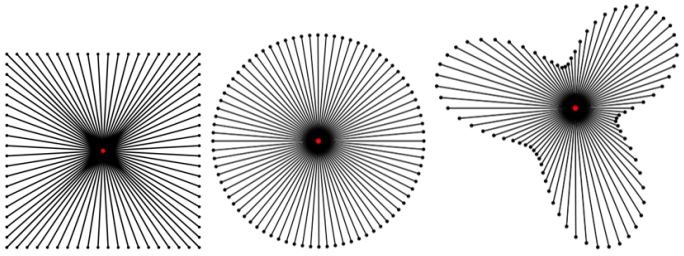

Fig. 2. Three actuators: s-PZT (left), c-PZT (center), a-PZT (right)

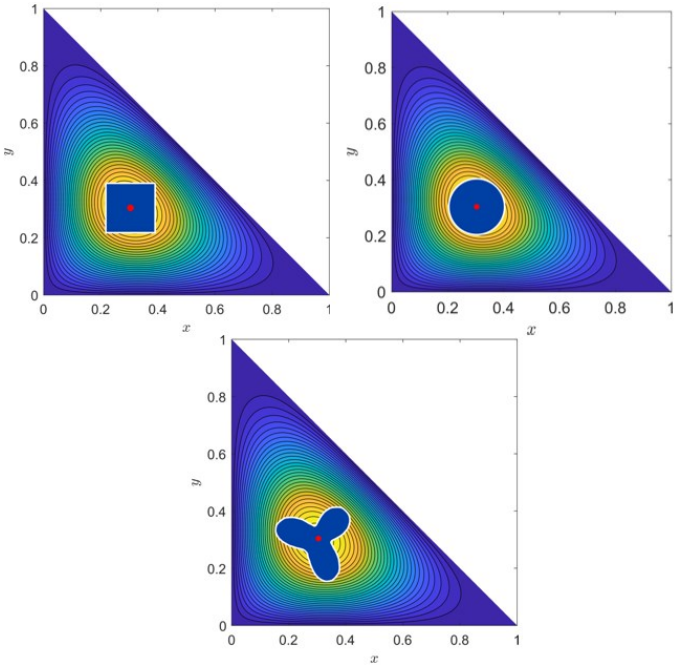

Fig. 3. The location of gluing the actuators on the plate surfaces

system by measuring (from the logarithmic decrement) the damping of adjacent, decreasing peaks. It boils down to determining the upper envelope of the damped vibration signal, see Fig. 4,

$$\zeta = \frac{\delta}{\sqrt{\delta^3+(2\pi)^2}} \tag{13}$$

where $\delta = \ln\frac{x_0}{x_1}$, x_0 and x_1 are amplitudes of any two adjacent peaks.

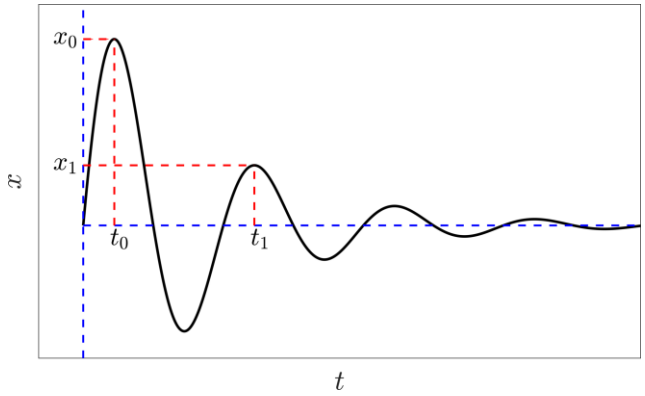

Fig. 4. Logarithmic decrement of an example function

IV. Calculating the Modal Viscous Damping Factor

Using modal analysis procedure, one can express the transverse displacement of the plate as [10],

$$w(x,y,t) = \sum_{n=1}^{\infty} w_n(x,y)\eta_n(t) \tag{7}$$

where $w_n(x,y)$ is the n-th mode shape of the plate and $\eta_n(t)$ denotes the generalized displacement. The mode shapes satisfy the orthogonality condition and can be normalized as follows,

$$\int_{\Omega} \varrho h w_n^2 dxdy = 1 \tag{8}$$

where Ω denotes triangular domain of the plate. By using the normalized mode shapes and substituting Eq. (7) to Eq. (1) one can obtain [10], [19],

$$\ddot{\eta}_n(t) + \omega_n^2\eta_n(t) = Q_n(t) \tag{9}$$

where $Q_n(t)$ is the generalized force and is given by,

$$Q_n(t) = \int_{\Omega} w_n(x,y) f(x,y,t) dxdy \tag{10}$$

Modal viscous damping factor ζ can be included in Eq. (9),

$$\ddot{\eta}_n(t) + 2\zeta\omega_n\dot{\eta}_n(t) + \omega_n^2\eta_n(t) = Q_n(t) \tag{11}$$

The damping represents numerous dissipation mechanisms in the structure. These mechanisms are generally poorly known. One of the damping hypotheses is called the Rayielgh hypothesis and it assumes that damping is proportional to the inertia and to the stiffness,

$$\zeta_n = \frac{1}{2}\left(\alpha\omega_n + \frac{\beta}{\omega_n}\right) \tag{12}$$

The paper assumes that ζ is proportional to inertia only. Hence, the ζ calculation procedure consists of determining the damping coefficient for the lowest natural frequency of the

V. Experimental Setup

The experimental setup consists of a laptop with MATLAB software, the NI USB-6212 Multifunction I/O Device with BNC connectors, a power amplifier and a laser-optical sensor (Fig. 5, 6). As part of this article, a program was created that generates a sine wave with a given amplitude and frequency with 10 kS/S sample rate. This signal goes to the NI device, then passes through the power amplifier and powers the actuator. Simultaneously, the measurement data is read by the optoNCDT optoelectronic sensor. The analog signal from the sensor is sent via the NI DAQ to the PC and the data is saved. The sensor measures plate vibrations with a sample rate up to 20 kS/s. The measuring range of the sensor is 2 mm. The program works in such a way that a sine wave is generated for 3 seconds, then the program pauses for 1 second. From the middle part of the data (between 1st and 2nd second) the amplitude of vibrations read from the sensor is calculated. At this point, the frequency of the sine wave supplying the actuator increases by the set value and the measurement cycle is repeated.

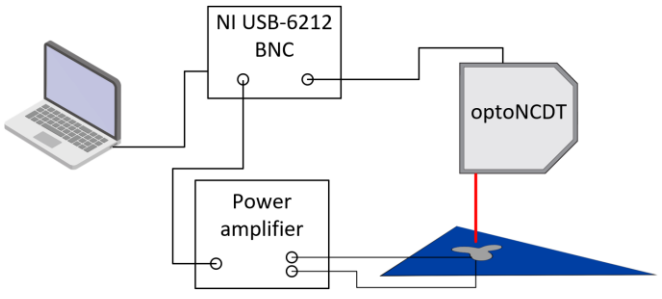

Fig. 5. Laboratory setup

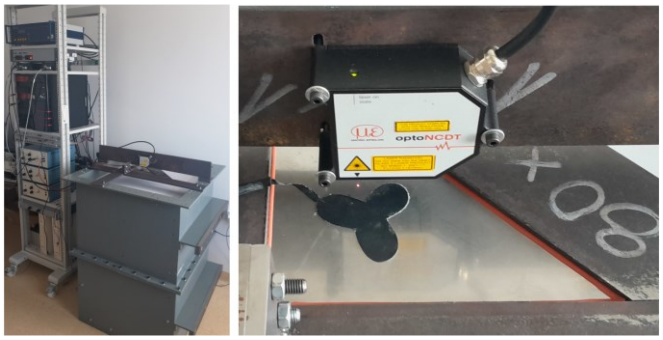

Fig. 6. The photographs of the laboratory setup.

Figure 7 shows an experimental realization of the simply supported boundary condition of the plate. All edges of the plate have been chamfered at 30-degree angle. The plate mounting consists of two parts and has been designed in such a way that, after screwing the two parts together, the plate lies simply supported in the 90-degree milled groove.

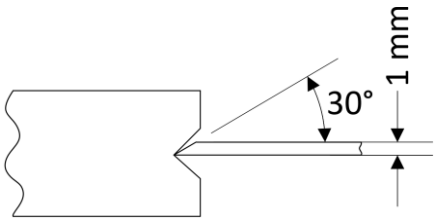

Fig. 7. Cross-section of the plate mounting and the plate that lies in the milled groove.

Figure 8 shows the three tested actuators. The actuators were designed on the basis of [9] and manufactured by Bimitech Inc. The transducers were glued to the surface of the plate with a two-component epoxy adhesive.

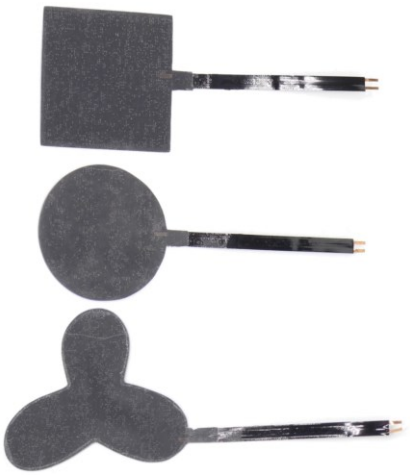

Fig. 8. Three tested PZTs: s-PZT (top), c-PZT (center), a-PZT (bottom).

Due to the fact that piezoelectric actuators must be glued to the structure in a permanent method, three identical 1 mm thick stainless steel plates were made for the purposes of the experiment. Thus, on one plate s-PZT was glued, on the other c-PZT, on the third a-PZT.

VI. Experimental Results

As part of the experiment, the modal viscous damping factor of the plate was calculated and the frequency response of each actuator acting in an open-loop control was determined.

A. Viscous Damping Ratio ζ

The viscous damping ratio was calculated for one of the plates. The plate with s-PZT was chosen. For this purpose, the frequency response for a narrower frequency range was collected. The measurement time was also extended so as to save the data after turning off the PZT to get the time interval in which the vibrations vanish.

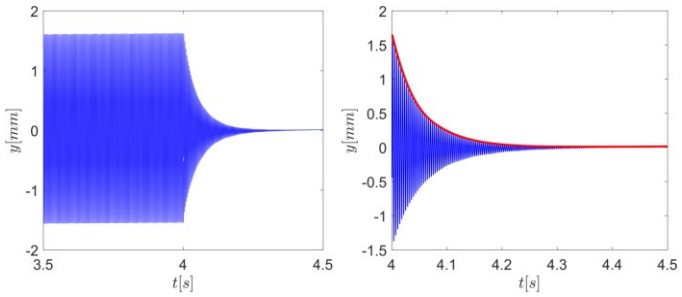

Fig. 9. Readout from the vibration sensor when using c-PZT (left) and envelope of the damped signal (right).

The β coefficient obtained from the interpolation of the signal envelope was determined and its value is β = 19.4955. Therefore, the viscous damping ratio ζ was calculated, the measurement was made for the frequency f = 278 Hz.

$$\zeta = \frac{\beta}{2\omega_n} = 5.5809 \text{ e-3} \qquad (14)$$

The frequency f = 278 Hz results from experimental identification of the model and this was the first natural frequency of the tested triangular plate.

B. Open-loop FRF

For each of the actuators, an open-loop frequency response was found between the voltage applied to the transducer and the voltage read by the sensor. The signal from the sensor corresponded to the transversal displacement of the plate at the same point for all of the plates.

Each of the actuators was supplied with the same voltage, then the frequency was changed by 1 Hz and the open loop amplitude was readout. The supply voltage for all three PZTs was 60 V.

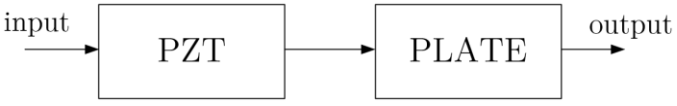

Fig. 10. Open-loop frequency response scheme.

Figure 11 shows the frequency response for the three tested actuators. The first resonant frequency was approx. 278 Hz for all plates, the lowest frequency response in the entire tested range was noted for the plate with c-PZT.

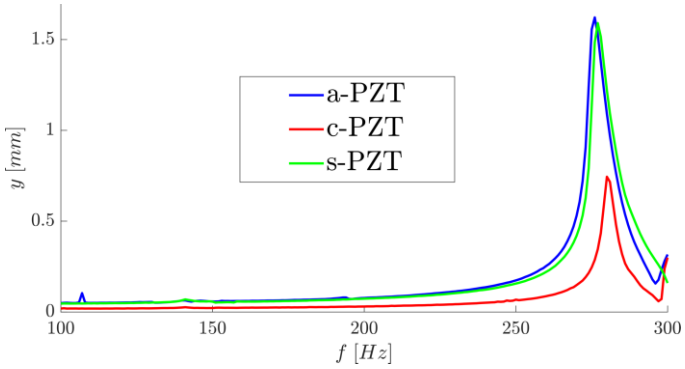

Fig. 11. Open-loop frequency response for the actuators.

In [9], the efficiency of the same actuators was investigated numerically for a steady state. The results were expressed in the vibration reduction coefficient, which was the difference between the largest amplitude without acting PZT and the amplitude after PZT acting, referred to the amplitude without active damping. This coefficient was expressed as a percentage. The results are as follows:

1) for a-PZT – 99.69 %
2) for c-PZT – 97.70 %
3) for s-PZT – 97.43 %

CONCLUSION

The paper describes the experimental studies of actuators of three different shapes applied to the active reduction of vibrations of a triangular plate. The article complements the theoretical considerations presented in previous publications and presents their experimental validation. Based on the research made, the following conclusions can be drawn:

1) The frequency response of a-PZT is greater in almost the entire range than the other actuators. Thus, it can be concluded that a-PZT is has the highest efficiency among the tested transducers.
2) The c-PZT has the smallest frequency response in the tested range. The efficiency of vibration reduction differs significantly from the efficiency obtained in [9]. This can be explained by the fact that each of the plates – although of the same dimensions and made in the same way – is slightly different from the others. Minimal changes related to the tolerance of the cutting device could affect the stability of the boundary conditions on part of the edge, which affected the results. In any case, this response is smaller than a-PZT, which makes c-PZT less effective.
3) Viscous damping ratio for the tested frequency was 5.5809e-3. This result is in line with the literature – $\zeta < 0.01$ for metals in elastic range [21].

The study confirms the justification of using a-PZT in the active reduction of plate vibrations and the need to optimize the shape of the actuator to achieve the highest efficiency of vibration reduction.

ACKNOWLEDGEMENTS

This research did not receive any specific grant from funding agencies in the public, commercial, or not-for-profit sectors.

REFERENCES

[1] W. Wang, *Electrode shape optimization of piezoelectric transducers*. Gainesville, 2003.

[2] X. Zhang, A. Takezawa, Z. Kang, ”Topology optimization of piezoelectric smart structures for minimum energy consumption under active control,” Structural and Multidisciplinary Optimization, vol. 58, pp. 185–199, 2018. https://doi.org/10.1007/s00158-017-1886-y

[3] L. Leniowska, D. Mazan, ”MFC Sensors and Actuators in Active Vibration Control of the Circular Plate,” Archives of Acoustics, vol. 40, no. 2, pp. 257-265, 2015. https://doi.org/10.1515/aoa-2015-0028

[4] J. Rzepecki, A. Chraponska, K. Mazur, S. Wrona, M. Pawełczyk, ”Semi-active reduction of device casing vibration using a set of piezoelectric elements,” in 2019 20th International Carpathian Control Conference (ICCC), 2019, pp. 1-5. https://doi.org/10.1109/CarpathianCC.2019.8765993

[5] A. Donoso, O. Sigmund, ”Optimization of piezoelectric bimorph actuators with active damping for static and dynamic loads,” Structural and Multidisciplinary Optimization, vol. 38, pp. 171–183, 2009. https://doi.org/10.1007/s00158-008-0273-0

[6] R. Trojanowski, J. Wiciak, ”Impact of the size of the sensor part on sensor-actuator efficiency,” Journal of Theoretical and Applied Mechanics, vol. 58, no. 2, pp. 391-401, 2020. https://doi.org/10.15632/jtam-pl/118948

[7] R. Trojanowski, J. Wiciak, ”Piezoelectric Square Based Sensor-actuator Hybrid in Vibration Reduction,” Vibrations in Physical Systems, vol. 33, no. 3, 2022. http://doi.org/10.21008/j.0860-6897.2022.3.03

[8] A. Branski, R. Kuras, ”Asymmetrical PZT Applied to Active Reduction of Asymmetrically Vibrating Beam – Semi-Analytical Solution,” *Archives of Acoustics*, vol. 47, no. 4, pp. 555–564, 2022. https://doi.org/10.24425/aoa.2022.142891

[9] A. Branski, R. Kuras, ”PZT Asymmetrical Shape Optimization in Active Vibration Reduction of Triangular Plates,” *Archives of Acoustics*, vol. 48, no. 3, pp 425-432, 2023. https://acoustics.ippt.pan.pl/index.php/aa/article/view/3740

[10] S. S. Rao, *Vibration of Continuous Systems*. Hoboken: John Wiley & Sons Inc., 2007.

[11] A. W. Leissa, *Vibration of plates*, Washington: Scientific and Technical Information Division NASA, 1969.

[12] D. J. Gorman, *Vibration analysis of Plates by the Superposition Method*. Singapore: World Scientific Publishing Co. Pte. Ltd., 1999.

[13] D. J. Gorman, ”A highly accurate analytical solution for free vibration analysis of simply supported right triangular plates,” *Journal of Sound and Vibration*, vol. 89, no. 1, pp. 107–118, 1983. https://doi.org/10.1016/0022-460X(83)90914-8

[14] H. T. Saliba, ”Transverse free vibration of simply supported right triangular thin plates: a highly accurate simplified solution,” *Journal of Sound and Vibration*, vol. 139, no. 2, pp. 289–297, 1990. https://doi.org/10.1016/0022-460X(90)90889-8

[15] H. T. Saliba, ”Free vibration of simply supported general triangular thin plates: an accurate simplified solution,” *Journal of Sound and Vibration*, vol. 196, no. 1, pp. 45–57., 1996. https://doi.org/10.1006/jsvi.1996.0466

[16] A. Branski, S. Szela, ”Improvement of effectiveness in active triangular ´ plate vibration reduction,” Archives Of Acoustics, vol. 33, no. 4, pp.521–530, 2008. https://acoustics.ippt.pan.pl/index.php/aa/article/view/549/480

[17] A. Branski, S. Szela, ”Quasi-optimal PZT distribution in active vibration reduction of the triangular plate with P-F-F boundary conditions,” Archives of Control Sciences, vol 20, no. 2, pp. 209-226, 2010. https://doi.org/10.2478/v10170-010-0014-7

[18] S.-C. Her, H.-Y. Chen, ”Deformation of Composite Laminates Induced by Surface Bonded and Embedded Piezoelectric Actuators,” Materials, vol. 13, no. 14, 2020. https://doi.org/10.3390/ma13143201

[19] A. Premount, *Vibration Control of Active Structures*, Berlin: Springer, 2011.

[20] R. Kuras, ”Influence of the PZT Actuator Asymmetry on the LQR Control Parameters in the Active Reduction Vibrations of Beams,” Vibrations in Physical Systems, vol. 33, no. 3, 2022. https://doi.org/10.21008/j.0860-6897.2022.3.05

[21] V. Adams, A. Askenazi, *Building Better Products with Finite Element Analysis*, Santa Fe: OnWord Press, 1999.